

Room-Temperature Low-Field Colossal Magnetoresistance in Double-Perovskite Manganite

S. Yamada,¹ N. Abe,² H. Sagayama,^{3,4} K. Ogawa,¹ T. Yamagami,¹ and T. Arima²

¹*Department of Materials System Science, Yokohama City University, Yokohama 236-0027, Japan*

²*Department of Advanced Materials Science, The University of Tokyo, Kashiwa 277-8561, Japan*

³*Institute of Materials Structure Science, High Energy Accelerator Research Organization, Tsukuba, Ibaraki 305-0801, Japan*

⁴*Department of Materials Structure Science, The Graduate University for Advanced Studies, Tsukuba, Ibaraki 305-0801, Japan*



(Received 11 January 2019; published 17 September 2019)

We have discovered room-temperature low-field colossal magnetoresistance (CMR) in an *A*-site ordered NdBaMn₂O₆ crystal. The resistance changes more than 2 orders of magnitude at a magnetic field lower than 2 T near 300 K. When the temperature and magnetic field sweep from an insulating (metallic) phase to a metallic (insulating) phase, the insulating (metallic) conduction changes to the metallic (insulating) conduction within 1 K and 0.5 T, respectively. The CMR is ascribed to the melting of the charge and orbital ordering. The entropy change which is estimated from the *B*-*T* phase diagram is smaller than what is expected for the charge and orbital ordering. The suppression of the entropy change is attributable to the loss of the short-range ferromagnetic fluctuation of Mn spin moments, which is an important key of the high temperature and low magnetic field CMR effect.

DOI: 10.1103/PhysRevLett.123.126602

Colossal magnetoresistance (CMR) [1–9] in a series of perovskite manganites RE_{1-x}AE_xMnO₃ (where RE is a trivalent rare earth and AE a divalent alkaline earth metal) has attracted much attention for decades. The drastic phenomena are caused by the strong coupling among charge, orbital, and spin degrees of freedom. The negative magnetoresistance phenomena in perovskite manganites are classified into two categories. A fairly gradual and rather moderate negative magnetoresistance was observed around room temperature in La_{1-x}Sr_xMnO₃ [5,6]. This reduction of resistance is attributed to the gradual increase in the bandwidth by aligning the Mn spins in a magnetic field that is often referred to as the double-exchange mechanism. As a result, the change in resistivity is also gradual and a high magnetic field of 5 T is needed to decrease the resistivity by one order. Another type of CMR effect, which is caused by the melting of charge ordering, was discovered in many compounds like Pr_{1-x}Ca_xMnO₃ [7,8]. The charge-order melting-type CMR is much larger and steeper than that of the pure double-exchange type. For example, the resistivity in (Nd_{0.06}Sm_{0.94})_{1/2}Sr_{1/2}MnO₃ at 115 K changes by more than 2 orders of magnitude in a low magnetic field below 1 T [10]. The magnetic field necessary for a one-order decrease in resistivity is about 0.2 T. However, the CMR of charge-order melting type in manganese oxide compounds has been rarely observed at room temperature so far, because the charge-ordering phase-transition temperature is lower than room temperature in most cases. Although some perovskite manganite compounds like Bi_{1-x}Sr_xMnO₃ [11–14] and REBaMn₂O₆ (RE = Sm-Y) [15–28] exhibit the charge-ordering phase

above room temperature, such charge-ordering phases are robust in a moderate magnetic field. In Sm_{1-x}La_{x+y}Ba_{1-y}Mn₂O₆ [26], which exhibits the room-temperature CMR effect by melting the charge-ordering phase, for example, a magnetic field of 9 T is necessary for the resistivity to change by one order of magnitude. In this Letter, we report room-temperature CMR in a NdBaMn₂O₆ single crystal. Previous studies using polycrystalline samples revealed that the magnetic susceptibility suddenly dropped with cooling across 290 K. This anomaly was attributed to the *A*-type (layered) antiferromagnetic ordering of Mn spin moments [20,22,24]. We recently succeeded in single-crystal growth of NdBaMn₂O₆ and proposed that a first-order metal-insulator phase transition should not be accompanied by any magnetic ordering [29]. The resistivity change upon the metal-insulator transition is still larger than 2 orders of magnitude. The metal-insulator transition temperature *T*_{MI} is decreased by applying a magnetic field. A high-quality single crystal exhibits the metal-insulator transition near 300 K. When temperature sweeps from insulating (metallic) phase to metallic (insulating) phase, the insulating (metallic) conduction changes to the metallic (insulating) conduction within 1 K. The crystal exhibits a room-temperature CMR effect at a relatively low field of 2 T.

Single crystals of NdBaMn₂O₆ were grown by a floating zone method, details of which were published elsewhere [29]. Magnetization was measured using a commercial superconducting quantum interface device magnetometer (Quantum Design MPML-XL). Electrical resistivity and magnetoresistance were measured using a commercial system (Quantum Design PPMS) by the conventional

four-probe method. For measuring the magnetic field dependence, the sample was warmed from 250 K to the target temperatures at 0 T. X-ray diffraction measurement on the single-crystal sample was performed using synchrotron radiation at the Photon Factory, High Energy Accelerator Research Organization, Japan. The dimensions of the single crystal sample were $1 \text{ mm} \times 1 \text{ mm} \times 2 \text{ mm}$. X-ray-diffraction intensities were collected by the oscillation photograph method with a cylindrical imaging-plate diffractometer at BL-8B. The collected data were analyzed by RAPID AUTO (Rigaku Co.). The temperature was controlled by using a He-gas spray-type refrigerator. The wavelengths were selected to be 0.688 \AA . Latent heat of a $\text{NdBaMn}_2\text{O}_6$ single crystal of 17 mg was measured using a commercial differential scanning calorimeter (Hitach Hightech DSC-7020) with a reference sample of Al_2O_3 . The sweeping rate of temperature was set 3 K/min.

Figure 1 shows temperature dependence of intensities of x-ray superlattice reflections, electrical resistivity, and magnetization of $\text{NdBaMn}_2\text{O}_6$ single crystal. The magnetization and resistivity show an anomaly near $T_{\text{MI}} = 300 \text{ K}$ in the warming run. In a magnetic field of 7 T, the phase-transition temperature in the warming run decreases to 283 K. The insulating phase between 283 and 300 K hence changes to the metallic phase by the application of a magnetic field. The resistivity change is more than 2 orders of magnitude. Because the resistivity does not depend on temperature very much either in the metallic or insulating phase, the magnitude of CMR is not sensitive to temperature. Though the phase transition is accompanied with a hysteresis, the resistivity change is very sharp. When temperature sweeps from the insulating (metallic) phase to the metallic (insulating) phase, the insulating (metallic) conduction changes to the insulating (metallic) conduction within 1 K. It is of note that the metallic and insulating phases coexist in the hysteresis. The metal-insulator transition is accompanied by a magnetic anomaly, as shown in Fig. 1(f). Though the magnetization above T_{MI} increases with a magnetic field, the magnetization below T_{MI} does not depend on a magnetic field very much. Single-crystal x-ray oscillation photographs indicate the charge and orbital ordering in the insulator phase below T_{MI} . All the x-ray reflections in this Letter are indexed on the basis of the $\sqrt{2}a_p \times \sqrt{2}a_p \times c_p$ unit cell, where a_p and c_p are lattice constants of the simple tetragonal unit cell, as shown in Fig. 1(a). The crystal contains *ab* twin structure as mentioned in our previous paper [29]. Only the fundamental reflections of the $\sqrt{2}a_p \times \sqrt{2}a_p \times c_p$ unit cell are observed above T_{MI} as shown in Fig. 1(c). In contrast, many superlattice reflections appear around 4 4 0 reflection below T_{MI} in Fig. 1(b). The superlattice reflections indicate that the unit cell below T_{MI} is $2\sqrt{2}a_p \times \sqrt{2}a_p \times 2c_p$. This unit cell is the same as that of the charge-ordering phase of $\text{SmBaMn}_2\text{O}_6$ between 200 and 380 K [30]. Here, it is of note that the intensities of the superlattice reflections are

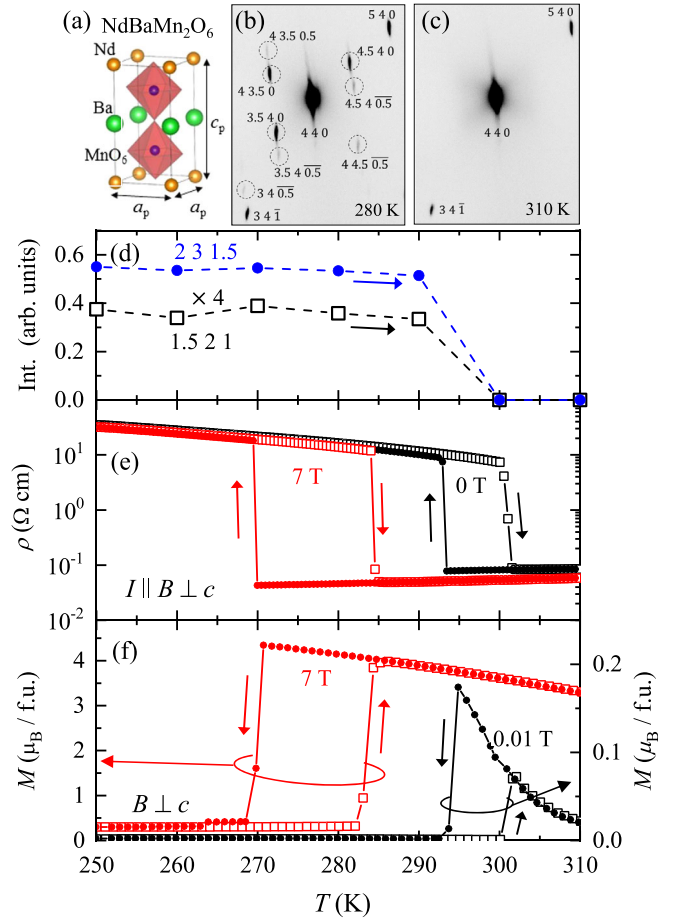


FIG. 1. X-ray oscillation photographs of a $\text{NdBaMn}_2\text{O}_6$ single crystal around 4 4 0 at (b) 280 K and (c) 310 K. The indices are given for the $\sqrt{2}a_p \times \sqrt{2}a_p \times c_p$ unit cell, where a_p and c_p are lattice constants of simple tetragonal unit cell shown in (a). Temperature dependence of (d) integrated intensities of 2 3 1.5 and 1.5 2 1 superreflections, (e) electrical resistivity at 0 T, and at 7 T, and (f) magnetization at 0.01 and 7 T. The magnetic field is applied perpendicular to the c axis, and parallel to the electric current in (e).

more than 6 orders weaker than some fundamental reflections. In our previous study [29], we used a crystal of a dimension $50 \mu\text{m} \times 10 \mu\text{m} \times 10 \mu\text{m}$ and could not detect superlattice reflections. In the present x-ray study we used a much larger crystal with a dimension of $1 \text{ mm} \times 1 \text{ mm} \times 2 \text{ mm}$. Then we could observe a series of superlattice reflections [31]. We have performed a neutron diffraction measurement on a single crystal and confirmed the absence of long-range magnetic order between 235 K and T_{MI} . Some previous studies by means of neutron powder diffraction measurements reported that Mn moments should be aligned to form the A-type antiferromagnetic order [20]. The checkerboard-type charge ordering is obviously inconsistent with the A-type antiferromagnetic ordering. The disagreement might be caused by some off-stoichiometry or A-site intermixing. A further neutron study would settle the problem.

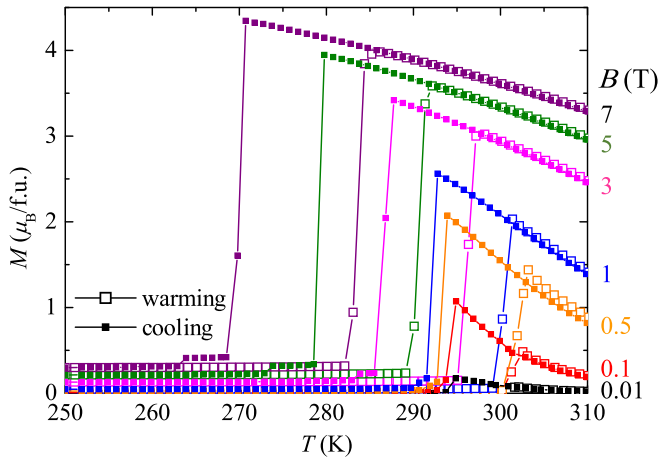


FIG. 2. Temperature dependence of magnetization. Open and solid squares denote warming and cooling runs, respectively. The magnetic field is applied perpendicular to the c axis.

Temperature dependence of magnetization at several magnetic fields is shown in Fig. 2. T_{MI} monotonically decreases with a magnetic field. The magnetization just above T_{MI} steeply increases with an applied magnetic field. This magnetization reaches $4.3 \mu_B/\text{f.u.}$ in the cooling run at 7 T. This value is much smaller than $7 \mu_B/\text{f.u.}$, the simple estimation of the fully saturated moment. Just below T_{MI} , the remnant magnetization and a small magnetization jump are observed only in a cooling run. The remnant magnetization could be attributed to a tiny portion of the charge disordered state, which would remain at the boundaries of ab twin domains. Since the behavior is only observed in magnetization but not transport data, we do not go into the detail in the present manuscript.

Magnetic field dependence of resistivity and magnetization around T_{MI} is shown in Fig. 3. At 310 K, which is just above T_{MI} , the resistivity slightly decreases with an increase of the magnetic field, while the magnetization steeply increases in a low magnetic field range. These results imply the presence of ferromagnetic fluctuation above T_{MI} , as reported in our previous paper [32]. The relative resistivity change at a magnetic field B is often defined as

$$\frac{\rho(0) - \rho(B)}{\rho(B)}. \quad (1)$$

This value is as small as 35% at 7 T, 310 K. At 297 K, which is just below T_{MI} , a metamagnetic transition which is accompanied with a metal-insulator phase transition is clearly observed. The relative resistivity change at 7 T exceeds 14 000%. This value is ten times as large as that of $\text{Sm}_{1-x}\text{La}_{x+y}\text{Ba}_{1-y}\text{Mn}_2\text{O}_6$ at 9 T at 300 K [26]. The resistivity change is very sharp. For example, at 297 K around the phase transition, the resistivity starts decreasing steeply at 1.9 T in a field increasing run, and the value of the resistivity at 2.1 T is more than one order of magnitude

smaller than that at 1.9 T as shown in the inset of Fig. 3(b). The steep change is almost finished at 2.4 T. The resistivity change with sweeping the magnetic field is as steep as that in $(\text{Nd}_{0.06}\text{Sm}_{0.94})_{1/2}\text{Sr}_{1/2}\text{MnO}_3$ at 115 K [10]. The phase-transition field increases with cooling. At 297 K, the insulator phase never revives just by sweeping the external magnetic field, if the field-induced insulator-to-metal transition once takes place. In contrast, at 290 K, the magnetic-field-induced insulator-metal transition becomes reversible. The steepness of the resistivity change in a magnetic field decreasing run is almost the same as that in a magnetic field increasing run. At 250 K, the insulator-metal transition is not observed up to 7 T and the relative resistivity change at 7 T is as small as 10%.

Next, we discuss the necessary condition for the low-field CMR at a wide temperature range. The Clausius-Clapeyron equation for a first-order magnetic phase transition is given as

$$\frac{dT_c}{dB} = -\frac{\Delta M}{\Delta S}, \quad (2)$$

where T_c , ΔM , and ΔS are the phase-transition temperature, difference in magnetization between two phases, and the entropy change upon the phase transition, respectively. Figure 4(a) shows the phase diagram on the magnetic field temperature plane. Because the present metamagnetic transition is accompanied with a hysteresis, the thermally equilibrium phase boundary cannot exactly be determined experimentally. Here, we assume that thermally equilibrium T_c is as high as average of the experimentally obtained T_{MI} 's in the warming and cooling runs at a constant magnetic field. The magnetic field dependence of T_{MI} is fitted by a quadratic function of a magnetic field B (a broken line in Fig. 4) [33]. Then we calculate ΔS from Eq. (2). The ΔS values are 4–7 J/(mol K) above 1 T [34]. ΔS at zero magnetic field is calculated from the latent heat, shown in Fig. 4(b), to be about 7 J/(mol K). The change in entropy estimated by taking only the charge and orbital sectors into account is larger than the measured value. We propose that the difference should be attributed to the spin sector. In the charge disordering phase, the entropy in the charge and orbital sectors in the doubly degenerate e_g orbitals is roughly estimated as $(3N_{\text{Mn}}/2)k_B \ln 2 \simeq 17.3 \text{ J}/(\text{mol K})$, where N_{Mn} and k_B are the number of Mn atoms in one molar $\text{NdBaMn}_2\text{O}_6$ and Boltzmann constant, respectively. The entropy in the charge and orbital sectors is about 10 J/(mol K) larger than the measured value of the entropy change. The change in Mn spin states should also attribute to the entropy change. Above T_{MI} , the short-range ferromagnetic contribution is enhanced with approaching T_{MI} , and suddenly disappears below T_{MI} . The Mn spin moments remain paramagnetic between Néel temperature (235 K) and T_{MI} [29]. In other words, the entropy in the spin sector increases with cooling across T_{MI} . In the paramagnetic phase,

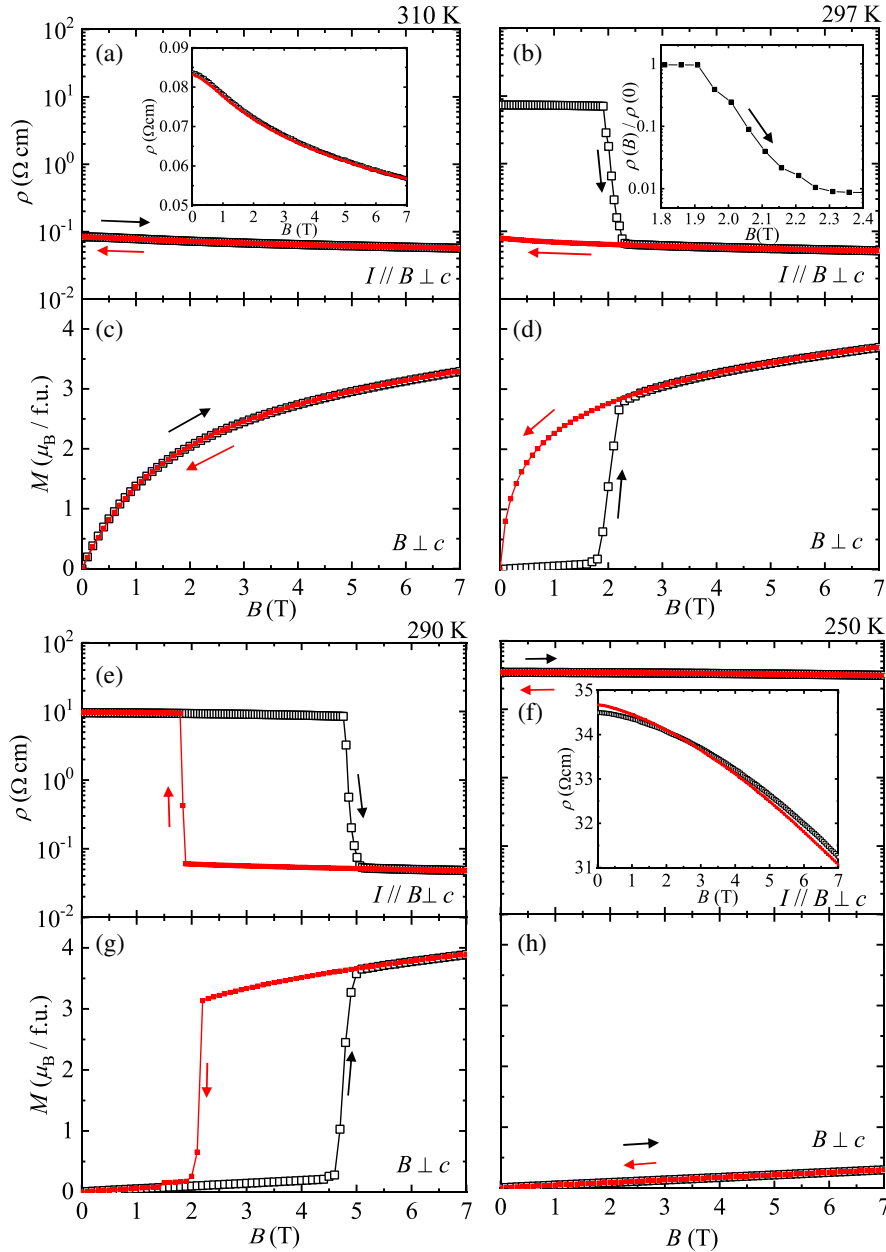


FIG. 3. Magnetic field dependence of (a),(b),(e),(f) resistivity and (c),(d),(g),(h) magnetization at several temperatures. Insets in (a) and (f) are (a) and (f) whose vertical scales are linear, respectively. The inset in (b) is an enlarged figure in the increasing run of a magnetic field in (b) around the metal-insulator transition. The resistivity of the inset in (b) is normalized by the resistivity at zero magnetic field (see text).

the spin entropy is estimated to be $(N_{\text{Mn}}/2)k_B \ln(5 \times 4) \simeq 24.9 \text{ J}/(\text{mol K})$ by neglecting the Mn spin correlation. If we neglect the change of lattice entropy upon the phase transition, the spin entropy above T_{MI} is roughly calculated to be about $15 \text{ J}/(\text{mol K})$. This value could be explained by assuming the formation of ferromagnetic clusters of 7–8 $\text{Mn}^{3.5+}$ ions above T_{MI} [35]. The low magnetic field CMR of $\text{NdBaMn}_2\text{O}_6$ should be closely related to the competition between the charge and orbital sectors and the spin sectors. The CMR effect in a low magnetic field in a wider temperature range can be realized by a further increase in $\Delta M/\Delta S$. If the

ferromagnetic cluster above T_{MI} becomes larger, it is expected that the operating magnetic field of the CMR effect becomes lower in a wide temperature range because both the enhancement of ΔM and the suppression of ΔS are satisfied simultaneously.

The above mentioned discussion suggests the necessary conditions for the high-temperature low-field CMR effect in the manganese oxide compounds. First, the charge-orbital ordering temperature T_{COO} must be high, because the charge-order melting-type CMR can only appear below T_{COO} . Second, ferromagnetic ordering or fluctuation must

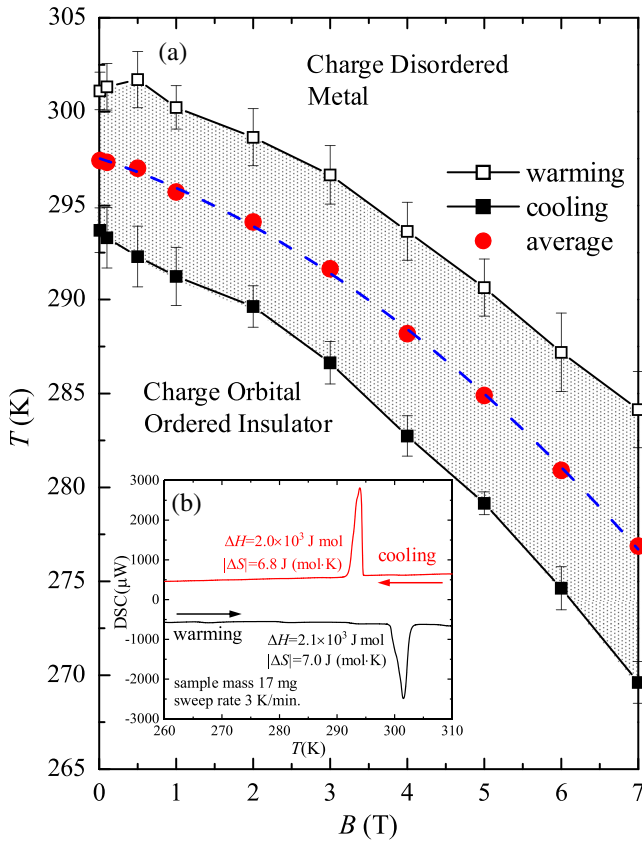


FIG. 4. (a) Phase diagram of $\text{NdBaMn}_2\text{O}_6$ in the magnetic field temperature plane. Solid circles show the average values of T_{MI} 's for cooling (open squares) and warming (solid squares) runs. The broken line is a fitting curve to the magnetic field dependence of the averaged T_{MI} (see text). (b) Differential scanning calorimetry around T_{MI} .

be present above T_{COO} for large ΔM . Third, the charge-orbital order phase just below T_{COO} must not be accompanied by antiferromagnetic ordering for a partial cancellation of a large entropy change in the charge and orbital sectors. In general, the first and second conditions are difficult to satisfy simultaneously. When the Mn—O—Mn bond angle is close to 180° , the ferromagnetic and metallic behavior becomes dominant due to the large double-exchange interaction. When the bond angle becomes smaller, antiferromagnetic and insulating behavior becomes dominant because of the suppression of the transfer of the e_g electron. In other words, if the charge-ordering phase is stable up to high temperatures, the ferromagnetic interaction would not survive above the charge-ordering phase-transition temperature. However, in $\text{NdBaMn}_2\text{O}_6$, the charge-ordering transition temperature reaches room temperature, while the $\text{NdBaMn}_2\text{O}_6$ has a large instability of ferromagnetism. In double perovskite manganites, random potential, which is harmful for any ordering, can be minimized. Furthermore, the average valence of Mn ions can be set to 3.5 exactly, which would favor the charge orbital ordering. The anisotropic crystal

structure may also assist the formation of orbital ordering. As a result, the charge-orbital order can be stabilized even if the e_g electron transfer energy is fairly large. Here, the alternate arrangement of RE and Ba would be essential for the reduction of the random potential. Nakajima *et al.* [23] showed that the enhancement of ordering ratio between RE and Ba atoms should raise T_{MI} and sharpen the transition. The intersite mixing between Nd and Ba in a single crystal with T_{MI} of 290 K in the warming run is estimated to be 1.2% by using single crystal structure analysis by means of the synchrotron x-ray diffraction measurements [29]. In the present study, T_{MI} is higher than 290 K, suggesting highly ordered A-site cations. Although the metal-insulator transition is accompanied with a large hysteresis for temperature and a magnetic field dependence due to the first-order nature of the transition, the resistivity changes for temperature and a magnetic field sweeping are very steep. This result means that the spatial randomness due to the intersite mixing between Nd and Ba strongly affects not only the stability of the charge and orbital ordering but also the steepness of the resistivity change with the phase transition. Once some nucleation happens in a crystal, the embryos can grow rapidly without heavy pinning of domain walls. Moreover, the resistivity change of the single crystal at the phase transition is steeper than that of the polycrystalline sample [22] due to the absence of the grain boundary resistance. The steepness of the resistivity change at the phase transition in the $\text{NdBaMn}_2\text{O}_6$ single crystals used in the present study would propose the almost complete removal of randomness.

In conclusion, colossal magnetoresistance (CMR) more than 2 orders of magnitude at a magnetic field lower than 2 T has been observed near 300 K in $\text{NdBaMn}_2\text{O}_6$ single crystal. The magnitude does not depend on temperature very much. Single crystal synchrotron x-ray diffraction has revealed that the insulating state below 300 K should be ascribed to the charge and orbital ordering. The charge-ordering phase near room temperature is melted by a relatively low magnetic field. Although the phase transition is accompanied with a large hysteresis, the resistivity steeply changes in temperature and magnetic field sweeping. Such a steepness of the resistivity change at the phase transition could be attributed to the almost complete removal of randomness by highly ordered Nd and Ba atoms.

This study was partly supported by a Grant-in-Aid for Scientific Research (No. 1818K03546) from the Japan Society for the Promotion of Science and by the grant for Strategic Research Promotion (No. G2503) of Yokohama City University. This work was performed under the approval of the Photon Factory Program Advisory Committee (Proposal No. 2014G597). Magnetoresistance measurements were performed using the facilities of the Institute for Solid State Physics, the University of Tokyo. Preliminary neutron diffraction measurement on a single crystal was performed at the Japan Proton Accelerator Research Complex (No. 2018B0174).

- [1] R. M. Kusters, J. Singleton, D. A. Keen, R. McGreevy, and W. Hayes, *Physica (Amsterdam)* **155B**, 362 (1989).
- [2] K. Chahara, T. Ohno, M. Kasai, and Y. Kozono, *Appl. Phys. Lett.* **63**, 1990 (1993).
- [3] R. von Helmolt, J. Wecker, B. Holzapfel, L. Schultz, and K. Samwer, *Phys. Rev. Lett.* **71**, 2331 (1993).
- [4] S. Jin, T. H. Tiefel, M. McCormack, R. A. Fastnacht, R. Ramesh, and L. H. Chen, *Science* **264**, 413 (1994).
- [5] Y. Tokura, A. Urushibara, Y. Moritomo, T. Arima, A. Asamitsu, G. Kido, and N. Furukawa, *J. Phys. Soc. Jpn.* **63**, 3931 (1994).
- [6] A. Urushibara, Y. Moritomo, T. Arima, A. Asamitsu, G. Kido, and Y. Tokura, *Phys. Rev. B* **51**, 14103 (1995).
- [7] Y. Tomioka, A. Asamitsu, Y. Moritomo, and Y. Tokura, *J. Phys. Soc. Jpn.* **64**, 3626 (1995).
- [8] Y. Tomioka, A. Asamitsu, H. Kuwahara, Y. Moritomo, and Y. Tokura, *Phys. Rev. B* **53**, R1689 (1996).
- [9] Y. Tokura and Y. Tomioka, *J. Magn. Magn. Mater.* **200**, 1 (1999).
- [10] H. Kuwahara, Y. Moritomo, Y. Tomioka, A. Asamitsu, M. Kasai, R. Kumai, and Y. Tokura, *Phys. Rev. B* **56**, 9386 (1997).
- [11] J. L. García-Muñoz, C. Frontera, M. A. G. Aranda, C. Ritter, A. Llobet, L. Ranno, M. Respaud, J. Vanacken, and J. M. Broto, *J. Magn. Magn. Mater.* **242–245**, 645 (2002).
- [12] J. L. García-Muñoz, C. Frontera, M. A. G. Aranda, A. Llobet, and C. Ritter, *Phys. Rev. B* **63**, 064415 (2001).
- [13] J. Hejtmanek, K. Knížek, Z. Jirák, M. Hervieu, C. Martin, M. Nevřiva, and P. Beran, *J. Appl. Phys.* **93**, 7370 (2003).
- [14] S. Yamada, T. Matsunaga, E. Sugano, H. Sagayama, S. Konno, S. Nishiyama, Y. Watanabe, and T. H. Arima, *Phys. Rev. B* **75**, 214431 (2007).
- [15] T. Nakajima, H. Kageyama, and Y. Ueda, *J. Phys. Chem. Solids* **63**, 913 (2002).
- [16] A. J. Williams and J. P. Attfield, *Phys. Rev. B* **66**, 220405(R) (2002).
- [17] T. Arima, D. Akahoshi, K. Oikawa, T. Kamiyama, M. Uchida, Y. Matsui, and Y. Tokura, *Phys. Rev. B* **66**, 140408(R) (2002).
- [18] S. V. Trukhanov, I. O. Troyanchuk, M. Hervieu, H. Szymczak, and K. Bärner, *Phys. Rev. B* **66**, 184424 (2002).
- [19] I. O. Troyanchuk, S. V. Trukhanov, and G. Szymczak, *Crystallogr. Rep. (Transl. Kristallografiya)* **47**, 658 (2002).
- [20] T. Nakajima, H. Kageyama, H. Yoshizawa, K. Ohoyama, and Y. Ueda, *J. Phys. Soc. Jpn.* **72**, 3237 (2003).
- [21] H. Kageyama, T. Nakajima, M. Ichihara, Y. Ueda, H. Yoshizawa, and K. Ohoyama, *J. Phys. Soc. Jpn.* **72**, 241 (2003).
- [22] D. Akahoshi, M. Uchida, Y. Tomioka, T. Arima, Y. Matsui, and Y. Tokura, *Phys. Rev. Lett.* **90**, 177203 (2003).
- [23] T. Nakajima, H. Yoshizawa, and Y. Ueda, *J. Phys. Soc. Jpn.* **73**, 2283 (2004).
- [24] D. Akahoshi, Y. Okimoto, M. Kubota, R. Kumai, T. Arima, Y. Tomioka, and Y. Tokura, *Phys. Rev. B* **70**, 064418 (2004).
- [25] S. V. Trukhanov, L. S. Lobanovski, M. V. Bushinsky, V. V. Fedotova, I. O. Troyanchuk, A. V. Trukhanov, V. A. Ryzhov, H. Szymczak, R. Szymczak, and M. Baran, *J. Phys. Condens. Matter* **17**, 6495 (2005).
- [26] T. Nakajima and Y. Ueda, *J. Appl. Phys.* **98**, 046108 (2005).
- [27] S. V. Trukhanov, A. V. Trukhanov, H. Szymczak, R. Szymczak, and M. Baran, *J. Phys. Chem. Solids* **67**, 675 (2006).
- [28] S. V. Trukhanov, A. V. Trukhanov, H. Szymczak, C. E. Botez, and A. Adair, *J. Low Temp. Phys.* **149**, 185 (2007).
- [29] S. Yamada, H. Sagayama, K. Higuchi, T. Sasaki, K. Sugimoto, and T. Arima, *Phys. Rev. B* **95**, 035101 (2017).
- [30] H. Sagayama, S. Toyoda, K. Sugimoto, Y. Maeda, S. Yamada, and T. Arima, *Phys. Rev. B* **90**, 241113(R) (2014).
- [31] Some fundamental reflections were so strong that the data reached the saturation limit.
- [32] S. Yamada, H. Sagayama, K. Sugimoto, and T. Arima, *J. Phys. Conf. Ser.* **969**, 012103 (2018).
- [33] The function of the fitting curve is $T(B) = -0.233B^2 - 1.34B + 296$.
- [34] We also tried to fit the phase transition curve using an even and a quadratic function. However, the fitting curve does not represent the phase transition curve in both low and high magnetic field ranges. The function could be a higher order even function.
- [35] See Supplemental Material at <http://link.aps.org/supplemental/10.1103/PhysRevLett.123.126602> for the procedure of the estimation of the entropy.